REPORT DOCUMENTATION PAGE

Form Approved
OMB NO. 0704-0188

1. AGENCY USE ONLY *(Leave blank)*	2. REPORT DATE	3. REPORT TYPE AND DATES COVERED
	30 July 1998	Final Report

4. TITLE AND SUBTITLE

Molecular Assemblies on Oxide Surfaces

5. FUNDING NUMBERS

DAAH04-95-1-0144

6. AUTHOR(S)

Thomas J. Meyer

7. PERFORMING ORGANIZATION NAMES(S) AND ADDRESS(ES)

University of North Carolina
Chapel Hill, NC 27514

8. PERFORMING ORGANIZATION REPORT NUMBER

9. SPONSORING / MONITORING AGENCY NAME(S) AND ADDRESS(ES)

U.S. Army Research Office
P.O. Box 12211
Research Triangle Park, NC 27709-2211

10. SPONSORING / MONITORING AGENCY REPORT NUMBER

ARO 34094.4-CH

11. SUPPLEMENTARY NOTES

The views, opinions and/or findings contained in this report are those of the author(s) and should not be construed as an official Department of the Army position, policy or decision, unless so designated by other documentation.

12a. DISTRIBUTION / AVAILABILITY STATEMENT

Approved for public release; distribution unlimited.

12 b. DISTRIBUTION CODE

19981228 013

13. ABSTRACT *(Maximum 200 words)*

Our focus for the past 3 years has been on developing a fundamental understanding of the chemical and physical properties of metal complexes on metal oxide surfaces. Carboxylate or phosphonate binding to metal oxide substrates provides a basis for formation of monolayer or submonolayer coverages of molecular assemblies. We have obtained evidence for multiple binding sites on both ITO and TiO_2 transparent electrodes. We have also investigated the electrochemical response of these surface structures with regard to photovoltaic and electrocatalytic applications.

14. SUBJECT TERMS			15. NUMBER IF PAGES
			16. PRICE CODE
17. SECURITY CLASSIFICATION OR REPORT	18. SECURITY CLASSIFICATION OF THIS PAGE	19. SECURITY CLASSIFICATION OF ABSTRACT	20. LIMITATION OF ABSTRACT
UNCLASSIFIED	UNCLASSIFIED	UNCLASSIFIED	UL

Molecular Assemblies on Oxide Surfaces

Final Report

May 1, 1995 - April 30, 1998

July 30, 1998

U.S. Army Research Office

ARO Proposal Number 34094-CH

ARO Contract Number: G-DAAH04-95-1-0144

Department of Chemistry

University of North Carolina, Chapel Hill

Table of Contents

Abstract

Our focus for the past 3 years has been on developing a fundamental understanding of the chemical and physical properties of metal complexes on metal oxide surfaces. Carboxylate or phosphonate binding to metal oxide substrates provides a basis for formation of monolayer or submonolayer coverages of molecular assemblies. We have obtained evidence for multiple binding sites on both ITO and TiO_2 transparent electrodes. We have also investigated the electrochemical response of these surface structures with regard to photovoltaic and electrocatalytic applications.

In a related project, we have laid the ground work for understanding metal complexes immobilized in SiO_2 sol-gels films with regard to film stability and structure. These results have allowed us to pursue the use of these films in applications in catalysis and electroluminescence.

List of Manuscripts

Electropolymerization of Molecular Assemblies. Moss, J.A.; Argazzi, R.; Bignozzi, C.A.; Meyer, T.J. *Inorg. Chem.* **1997,** 36, 762-763

Excited State Interactions in Electropolymerized Thin Films of Ru^{II}, Os^{II} Zn^{II} Polypyridyl Complexes. Devenney, M.; Worl, L.A.; Gould, S.; Guadaupe, A.; Sullivan, B.P.; Caspar, J.V.; Leasure, R.L.; Gardner, J.R.; Meyer, T.J. *J. Phys. Chem.,* **1997**, 101, 4535-4540.

Ru(II) MLCT Excited States: Stabilization toward Ligand Loss in Rigid Media. Adelt, M.; Devenney, M.; Meyer, T.J.; Thompson, D.; Treadway, J., *Inorg. Chem.* **1998**, 37, 2616.

Sensitization of Nanocrystalline TiO_2 By Electropolymerized Thin Films. Moss, J.A.; Stipkala, J.M.; Yang, J.C.; Bignozzi, C.A.; Meyer, T.J., in press *Chemistry of Materials.*

Mechanisms of Surface Electron Transfer. Proton-Coupled Electron Transfer. Scott Trammell, John Wimbish and Thomas J. Meyer, submitted to *J. Am. Chem. Soc.*

Electron Transfer Catalysis of Surface Electron Transfer. Scott Trammell and Thomas J. Meyer, submitted to *Inorg. Chem.*

Kinetics of Absorbed Chromophore Exchange on Metal Oxide Electrodes. Scott Trammell and Thomas J. Meyer, manuscript in preparation.

Scientific Personnel Supported by this Grant

Thomas J. Meyer (Principal Investigator)

Martin Devenny (Post-doctoral Associate)

Scott Trammell (Post-doctoral Associate)

John Moss (Graduate Student) Ph.D. conferred

John Yang (Graduate Student)

Results

Below we summarize certain aspects of results of the past 3 years in our investigation of molecular assemblies on metal oxide surfaces. They can be grouped into two areas. In one, we have characterized the interaction of metal complexes containing carboxylate groups with metal oxide surfaces by designing simple exchange experiments. This study provided an understanding of the surface interaction, surface binding states and surface exchange dynamics. In the second, the focus was on exploiting these modified metal oxide surface in electrocatalysis, photovoltaics and electrochemiluminescence.

In one study a fundamental understanding of proton-coupled electron transfer was obtained for an anchored Ru catalyst on indium oxide. This result was instrumental in designing surfaces for the oxidation of organic substrates in electrocatalysis. In photovoltaics, stabilization of a Ru^{II} chromophore on TiO_2 was achieved by electropolymerizing "overlayers" of a Ru complex containing vinyl groups. With these results, we have been able to open a new approach to refine Grätzel-type photovoltaic cells with regard to stability with minimal loss of performance.

In a related project, we have laid the ground work for understanding metal complexes immobilized in SiO_2 sol-gels films with regard to film structure and retention in the films. These results have allowed us to design a second generation of film structures with respect to applications in catalysis and electroluminescence.

Metal Oxide Surfaces

Exchange Studies

We have investigated surface structures by the results of simple exchange experiments replacing $[Ru(bpy)_2(4,4'\text{-}(CO_2H)_2bpy)](PF_6)_2$ (**1**) for $[Os(bpy)_2(4,4'\text{-}(CO_2H)_2bpy)](PF_6)_2$ (**2**), (4,4'-$(CO_2H)_2$bpy is 4,4'-dicarboxy-2,2'-bipyridine) on a metal oxide surface.[1] One study explored the possible existence of more than one binding site on In_2O_3: Sn (ITO) optically transparent electrodes and on TiO_2 optically transparent ~6 μ thin films. On surfaces derivatized with **1**, adding **2** to the external solution in CH_3CN (or **2** for **1**) caused exchange of the initially bound complex within 2 hrs on ITO and within several days on TiO_2. After coming to equilibrium, the surface coverages, $\Gamma(mol/cm^2)$, were measured and the approach to equilibrium was analyzed by the Albery kinetic model.

The exchange study involved both equilibrium and kinetic studies. The kinetics of exchange are complex requiring multiexponential analysis consistent with a distribution of exchanging sites. In EtOH, a larger percentage of the sites undergo exchange compared to CH_3CN for both ITO and even more dramatically for TiO_2. The results of a series of equilibrium exchange studies are shown in Figure 1.

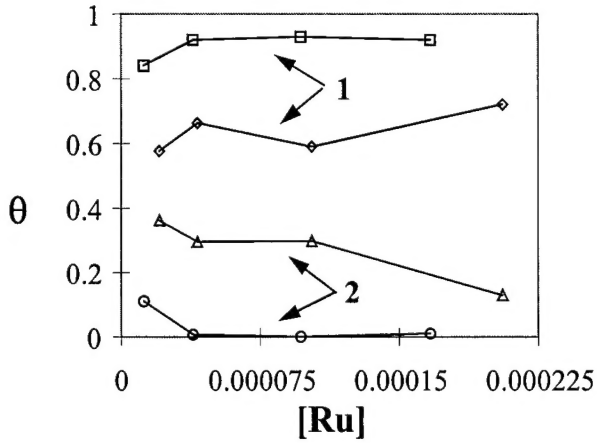

Figure 1. Fractional surface coverage, $\theta = \Gamma_t / \Gamma_0$, at equilibrium after exchanging **2** (Os^{II}) for **1** (Ru^{II}) on TiO_2 as a function of Ru^{II} in the external solution. $[Os(bpy)_2(4,4'\text{-}(CO_2H)_2bpy)](PF_6)_2$ (**2**) (Δ, CH_3CN; O, EtOH) and $[Ru(bpy)_2(4,4'\text{-}(CO_2H)_2bpy)](PF_6)_2$ (**1**) (◆, CH_3CN; ■, EtOH).

On ITO and TiO_2, the exchange kinetics in CH_3CN can be described by a dissociative model (eq 1). In eq 1, S- represents a surface site and Ru^{II} and Os^{II} are metal complexes **1** and **2**.

$$\mathbf{S\text{-}Ru^{II}} \underset{k_{-1}}{\overset{k_1}{\rightleftharpoons}} \mathbf{S\text{-} + Ru^{II}}$$

$$\mathbf{S\text{-} + Os^{II}} \underset{k_{-2}}{\overset{k_2}{\rightleftharpoons}} \mathbf{S\text{-}Os^{II}} \qquad (1)$$

The kinetics for this model are given by eq 2.

$$\frac{-d\theta_{Ru}}{dt} = \frac{d\theta_{Os}}{dt} = \frac{k_1 k_2 \theta_{Ru}[Os^{II}]}{k_{-1}[Ru^{II}] + k_2[Os^{II}]} \qquad (2)$$

With excess Os^{II}, in solution the exchange kinetics become pseudo first order in Os^{II} and,

$$\frac{-d\theta_{Ru}}{dt} = \frac{d\theta_{Os}}{dt} = k_{obs}\theta_{Ru} \qquad (3)$$

$$k_{obs} = \frac{k_1 k_2 [Os^{II}]}{k_{-1}[Ru^{II}] + k_2[Os^{II}]} \qquad (4)$$

The Albery kinetic model analyzes the exchange kinetics as a gaussian distribution of ln(k) values due to a distribution of exchanging sites with an average $\ln(\bar{k})$ defined by $\ln(k) = \ln(\bar{k}) + x\gamma$ ($-\infty \leq x \leq \infty$). The width of the distribution is γ and is ~3. In Figure 2 is shown an inverse-inverse plot consistent with eq 5, $k_1 \sim 0.1 s^{-1}$ and the ratio k_{-1}/k_2 ~5.2.

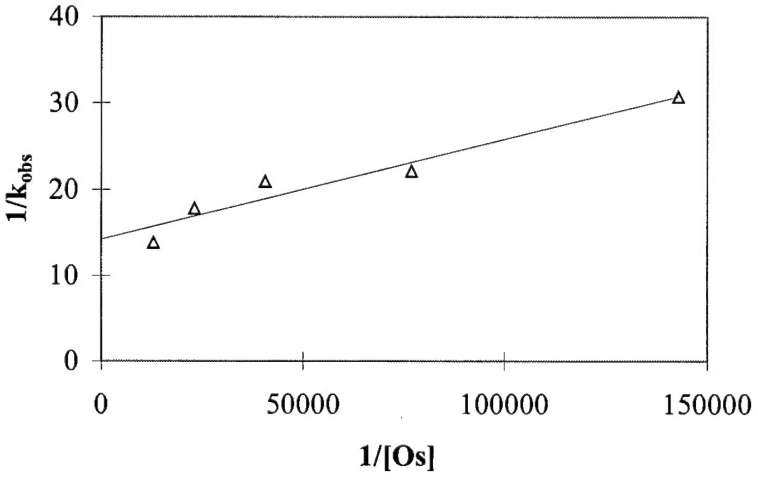

$$\frac{1}{k_{obs}} = \frac{k_{-1}[Ru]}{k_1 k_2 [Os]} + \frac{1}{k_1} \qquad (5)$$

Figure 2. Inverse inverse plot according to eq 5 with $[Ru^{II}] = 1.55 \times 10^{-6}$.

In EtOH, k_{obs} is independent of the concentration of the incoming metal complex, Os^{II} or Ru^{II}. This result is consistent with a dissociative model as in eq 1 but in which $k_1 << k_{-1}$, k_2 with EtOH labilizing the surface to exchange.

For the TiO_2 films, a similar analysis is obtained for exchange studies in CH_3CN and EtOH. However, the rate of exchange is much shower than at ITO. In this case, the rate of exchange is dependent on film thickness with thicker films having exchange rates that decrease with film thickness. This is consistent with hindered diffusion of the metal complexes through the TiO_2 matrix.

Electron Transfer Catalysis of Surface Electron Transfer

We have studied cross-surface electron transfer of the surface absorbed Ru^{II} and Os^{II} complexes $[Ru(bpy)_2(4,4'\text{-}(CO_2H)_2bpy)](PF_6)_2$ (**1**) and $[Os(bpy)_2(4,4'\text{-}(CO_2H)_2bpy)](PF_6)_2$ (**2**) and the catalysis of the surface couples by redox "carrier" couples in the external solution.[2]

In Figure 3 are shown a series of cyclic voltammograms of $[Os(bpy)_2(4,4'\text{-}(CO_2H)_2bpy)](PF_6)_2$ adsorbed on TiO_2 from CH_3CN (TiO_2-Os^{II}) which have been measured as a function of scan rate in 0.1 M TBAH in CH_3CN. In the insert is shown a plot of i_{pa} vs. $v^{1/2}$ showing the $v^{1/2}$ (v is scan rate) dependence expected for a diffusional process. ΔE_p ($\Delta E_p = E_{pa}\text{-}E_{pc}$) is significantly scan rate dependent varying from 275 mV at

v = 10 mV/s to 906 mV at v = 500 mV/s. The scan rate dependence demonstrates slow electron transfer.

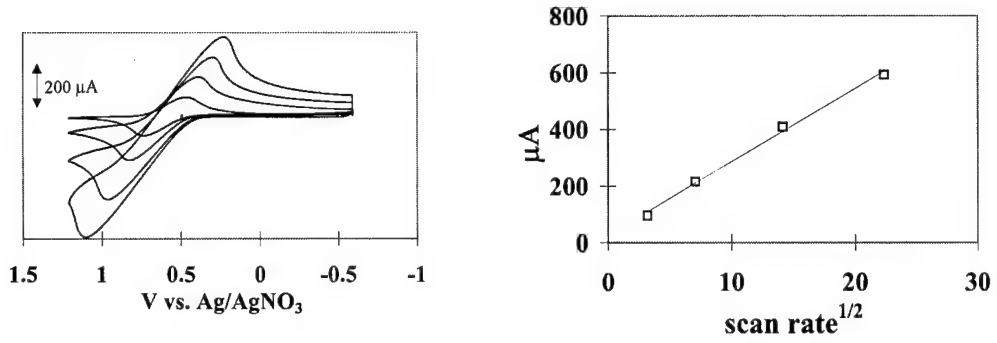

A **B**

Figure 3. Surface electrochemistry by cyclic voltammetry in 0.1M $[N(n\text{-}C_4H_9)_4](PF_6)$ in CH_3CN of a TiO_2 electrode loaded with $[Os(bpy)_2(4,4'\text{-}(CO_2H)_2bpy)]^{2+}$ from CH_3CN.

The dynamics of surface electron transfer were studied by chronoabsorptometry (absorbance monitoring following a potential step). A result from a chronoabsorptometry experiment for a TiO_2-Os^{II} electrode loaded from EtOH is illustrated in Fig 4a. The absorbance at 650 nm was monitored following potential steps first to 1300 mV vs. $Ag/AgNO_3$ which is past $E_{1/2}$ for Os (II→III) couple at 600 mV, and to 0 mV to observe Os (III→II) reduction. The double cycling process shows that electron transfer is reversible. For comparison, the result from a chronoabsorptometry experiment for a TiO_2-Os^{II} electrode from CH_3CN is illustrated in Fig 4b. To fully oxidize a TiO_2-Os^{II} electrode which had been loaded from EtOH takes nearly 1 hr. To fully oxidize a TiO_2-Os^{II} electrode loaded from CH_3CN takes less then 1 minute. Nearly twice the amount of

metal complex can be absorbed to TiO_2 from CH_3CN ($\Gamma_0 = 8.1 \times 10^{-8}$ mol/cm^2) as from EtOH ($\Gamma_0 = 5.7 \times 10^{-8}$ mol/cm^2) in 2×10^{-4} M solutions of metal complex.

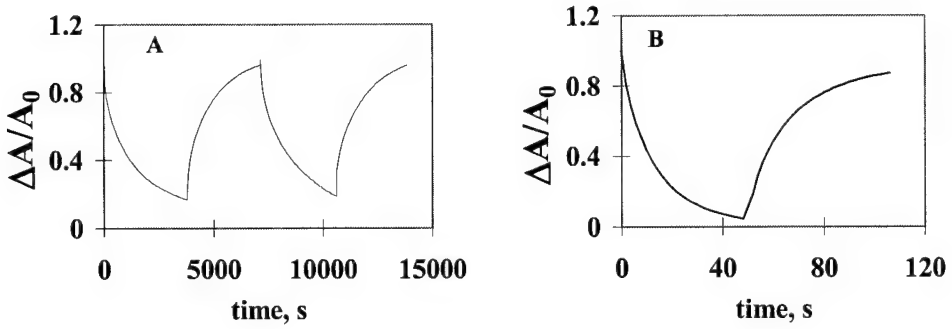

Figure 4 Time-dependent oxidation of $[Os^{II}(bpy)_2(4,4'\text{-}(CO_2H)_2)]^{2+}$ to Os^{III} on TiO_2 loaded from EtOH (A) compared to CH_3CN (B). The potential of the underlying ITO electrode was stepped to 1.3 V vs. $Ag/AgNO_3$ and absorption-time changes monitored at 650 nm.

The chronoabsorptometry experiments at early times show that the absorption changes follow the $t^{1/2}$ dependence predicted by the Cottrell equation, eq 6, which has be modified for chronoabsorptometry.

$$\Delta A / A_0 = \frac{2\varepsilon D_{app}^{\frac{1}{2}} t^{\frac{1}{2}}}{d\pi} \qquad (6)$$

In eq 6, ΔA is the change of absorbance of the adsorbed complex, ε_r the molar absorptivity, d is the film thickness, and A_0 is the initial film absorbance. The results are illustrated in figure 5.

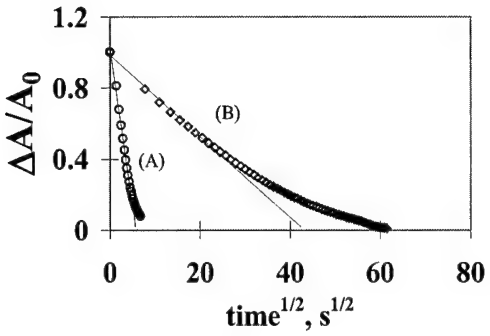

Figure 5. Time-dependent oxidation of $[Os^{II}(bpy)_2(4,4'\text{-}(CO_2H)_2)]^{2+}$ to Os^{III} on TiO_2 loaded from CH_3CN (A) compared to EtOH (B). The potential of the underlying ITO electrode was stepped to 1.3 V vs. $Ag/AgNO_3$ and absorbance-time changes monitored at 650 nm.

Table 1 Diffusion Coefficients for the Oxidation of TiO_2-Os^{II} loaded in Acetonitrile (AN0 or Ethanol (EtOH)

Electrode	[Ru] mM	D_{app} x 10^{-10} cm^2/s
Os-TiO_2 AN	0	280
Os-TiO_2 EtOH	0	0.90
"	0.0147	10.3
"	0.0441	37.6
"	0.0708	69.6
"	0.112	102

Similar results were obtained on ZrO_2. In Figure 6 are shown the results of a chronoabsorptometry experiment comparing a fully loaded film of $[Os^{II}(bpy)_2(4,4'\text{-}(CO_2H)_2)]^{2+}$ on ZrO_2 to a film diluted with $[Ru^{II}(bpy)_2(4,4'\text{-}(CO_2H)_2)]^{2+}$ by 33%. On the diluted surface electrochemistry of the $Os^{III/II}$ couple is nearly completely quenched.

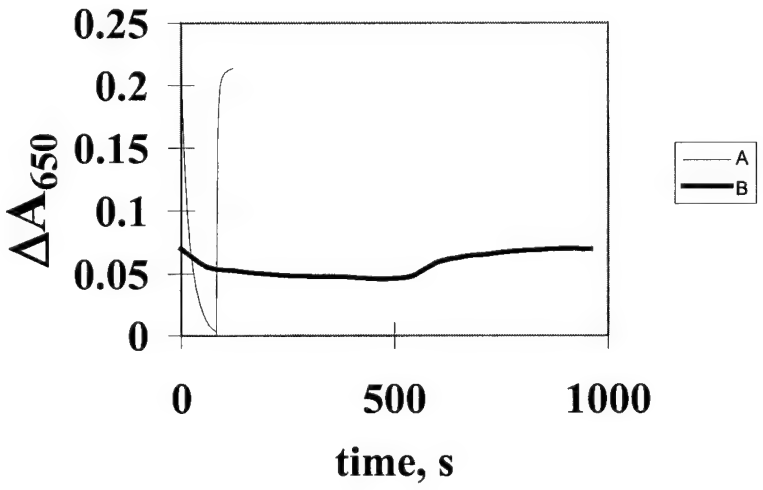

Figure 6. Time-dependent oxidation of $[Os^{II}(bpy)_2(4,4'\text{-}(CO_2H)_2)]^{2+}$ to Os^{III} on ZrO_2 loaded from CH_3CN (A) compared to a ZrO_2 surface diluted with $[Ru^{II}(bpy)_2(4,4'\text{-}(CO_2H)_2)]^{2+}$ (2:1) Ru^{II}:OsII. The potential of the underlying ITO electrode was stepped to 1.3 V vs. $Ag/AgNO_3$ and then to 0 V. Absorbance-time changes were monitored at 650 nm.

Catalysis of surface electron transfer for EtOH loaded films was investigated with added $Ru(bpy)_3^{2+}$ or $Os(bpy)_3^{2+}$ in the external solution. In Figure 7b is shown absorption vs. time plots for TiO_2-Os^{II} loaded from EtOH in the presence of 1.6×10^{-4} M $Ru(bpy)_3^{2+}$. The potential is stepped past the $Ru^{III/II}$ couple ($E_{1/2}$ =0.96 vs. $Ag/AgNO_3$) to 1.3 V and then to 0 V. There is a catalytic effect on the oxidative reaction but not the reductive reaction. An absorption vs. time plot for TiO_2-Os^{II} in the presence of 2×10^{-4} M Os^{II} is shown in Fig 7c. In this case the catalysis of the surface couple is greater for $Os^{III} \rightarrow Os^{II}$ reduction then for $Os^{II} \rightarrow Os^{II}$ oxidation. In Figure 7d, an absorption vs. time plot for TiO_2-Os^{II} in the presence of both $Ru(bpy)_3^{2+}$ and $Os(bpy)_3^{2+}$ is shown where both oxidation and reduction of the surface couple is enhanced.

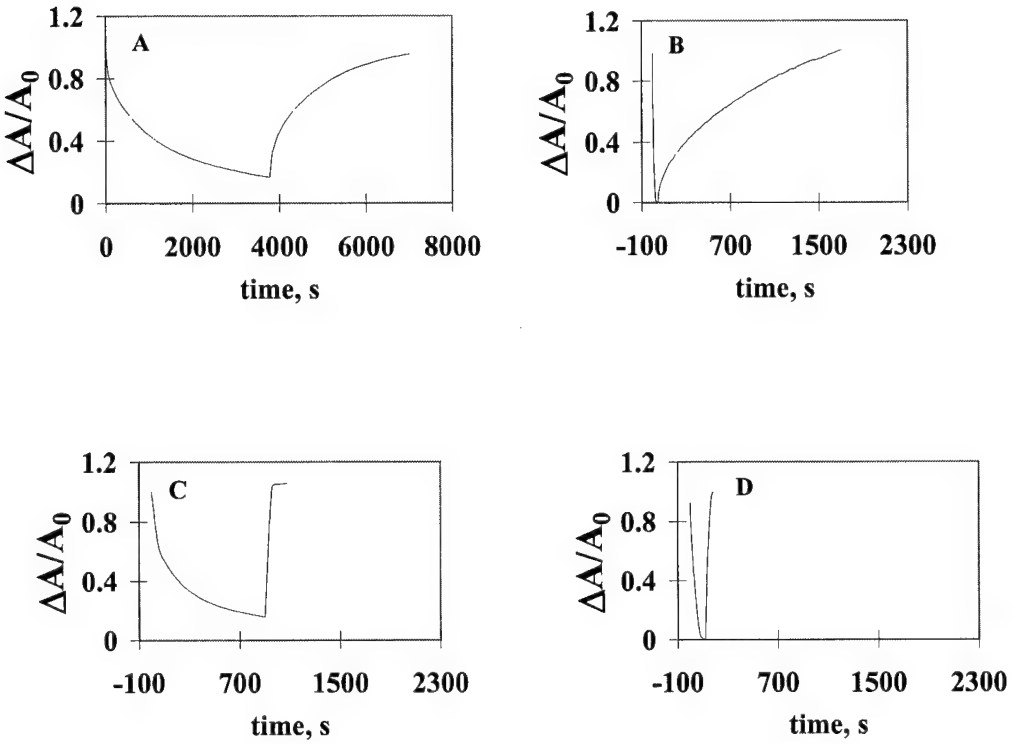

Figure 7. Time-dependent oxidation of $[Os^{II}(bpy)_2(4,4'\text{-}(CO_2H)_2)]^{2+}$ to Os^{III} on TiO_2 loaded from EtOH (A) compared to films catalyzed with added $Ru(bpy)_3^{2+}$ (B) or $Os(bpy)_3^{2+}$ (C) or both (D) in the external solution. The potential of the underlying ITO electrode was stepped to 1.3 V vs. $Ag/AgNO_3$ and then to 0 V and absorption time changes monitored at 650 nm.

The apparent diffusion coefficient, D_{app}, was calculated from the results of studies on the catalysis of surface electron transfer for EtOH loaded films in the presence of varying concentrations of $Ru(bpy)_3^{2+}$. In figure 8 is shown a plot of D_{app} vs. $[Ru^{II}]$ showing the linear relationship between them.

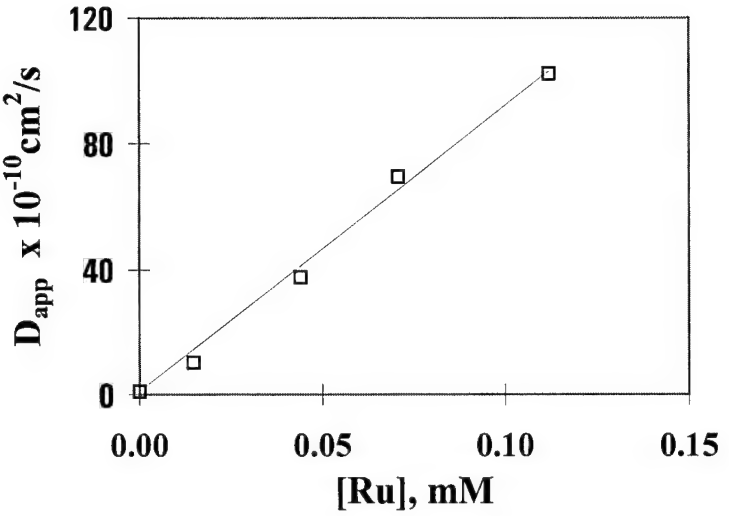

Figure 8. The apparent diffusion coefficient, D_{app} as a function of $[Ru(bpy)_3^{2+}]$ added as an "redox carrier" in the external solution.

These results are important in demonstrating the possible use of mobile redox carriers to catalysis of immobile redox couples for use in electrocatalysis in large surface area electrodes.

Proton-Coupled Surface Electron Transfer.

Oxidation-reduction reactions of redox-couples involving H^+ content changes between oxidation states such as such as $Ru^{IV}(tpy)(bpy)O^{2+}/Ru^{III}(tpy)(bpy)OH^{2+}/Ru^{II}(tpy)(bpy)OH_2^{2+}$ are often slow at electrode surfaces. Kinetic barriers are created from the requirement that electron transfer occur without change in proton content, at potentials higher than those for the thermodynamic couple. For example, for oxidation of $Ru^{II}(tpy)(bpy)(H_2O)^{2+}$, $E_{1/2}$ = 0.8 V vs. SSCE, the

$Ru^{III}(tpy)(bpy)(H_2O)^{3+/2+}$ couple independent of pH, while for the couple,

$$Ru^{III}(tpy)(bpy)(OH)^{2+} + H^+ + e^- \longrightarrow Ru^{II}(tpy)(bpy)(OH_2)^{2+} \quad (7)$$

$E_{1/2}$ =0.52 V vs. SSCE at pH 7.[3]

Recent reports have shown that it is possible to create relatively stable monolayer or submonolayer surface structures in aqueous solution by of phosphonate binding.[4] We have prepared stable surface structures based on the ligand 4,4'$(PO_3H_2)_2$bpy.[5]

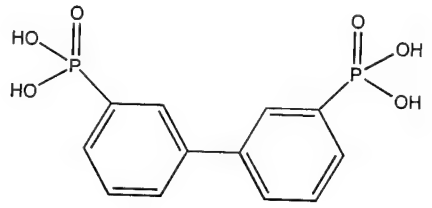

4,4'$(PO_3H_2)_2$bpy

Surface structures containing for [Ru(tpy)(4,4'$(PO_3H_2)_2$bpy)(H_2O)]$(ClO_4)_2$ on ITO are relatively stable for several hours in electrolyte of pH < 1 losing ~10% of coverage in the first hour of being exposed. At pH 7, the complex desorbs from the surface with a half life of ~30 minutes. At pH > 10, the complex desorbs from the surface within 10 minutes. Surface coverage follows a Langmuir isotherm with coverage reaching saturation in a solution of 2.2×10^{-4}M in metal complex with a final coverage of 0.8×10^{-10} mol/cm^2. From the Langmuir analysis, the formation constant for surface structure formation is K= 1.2×10^5 M^{-1}.

On the resulting absorbed structures, $E_{1/2}(Ru^{III/II})$ varies ~60mV/pH unit consistent with eq 7 as shown in Figure 9 from pH 1 to 10.8 and is identical to the $E_{1/2}(Ru^{III/II})$ measured in solution.

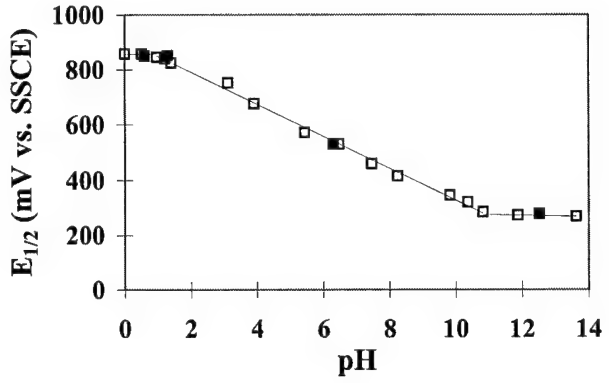

Figure 9. Plots of $E_{1/2}$ (V vs. SSCE) vs. pH for the $Ru^{III/II}$ redox couples of $[Ru(tpy)(4,4'(PO_3H_2)_2bpy)(H_2O)](ClO_4)_2$ on ITO, □ and in solution, ■. Recorded at a scan rate of 20 mV/s.

The electrode response is dependent on the extent of surface coverage. As shown in Figure 10, only the $Ru^{III/II}$ wave appears at $\Gamma \cong 0.3 \times 10^{-10}$ mol/cm^2 or 0.6×10^{-10} mol/cm^2 which are less than "monolayer" coverage. The $Ru^{IV/III}$ couple does appear on fully loaded surfaces, $\Gamma = 0.8 \times 10^{-10}$ mol/cm^2. Slow electron transfer is implied by the fact that the $Ru^{IV/III}$ couple appears only at scan rates ≤ 20mV/s. Significantly, as shown in Figure 11, the $Ru^{IV/III}$ wave does appear even on dilute surfaces if $[Ru(tpy)(bpy)(H_2O)]^{2+}$ is added to the external solution..

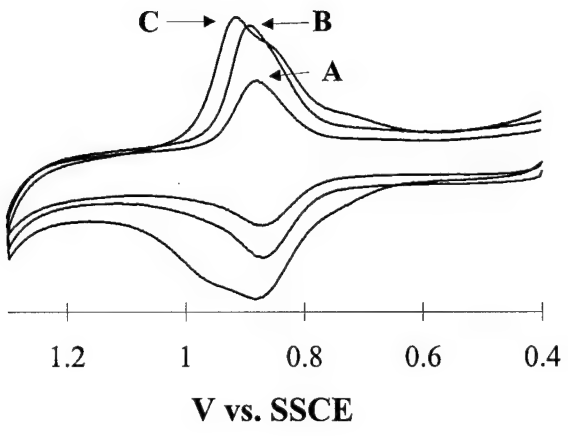

Figure 10. Cyclic voltammograms of $[Ru(tpy)(4,4'(PO_3H_2)_2bpy)(H_2O)](ClO_4)_2$ adsorbed on ITO at various surface coverages, $\Gamma(mol/cm^2)$. A) $\Gamma = 0.3 \times 10^{-10}(mol/cm^2)$, B) $\Gamma = 0.6 \times 10^{-10}(mol/cm^2)$ and at saturation, C) $0.8 \times 10^{-10}(mol/cm^2)$. The cyclic voltammograms were recorded in 0.1 M $HClO_4$ at a scan rate of 10 mV/s.

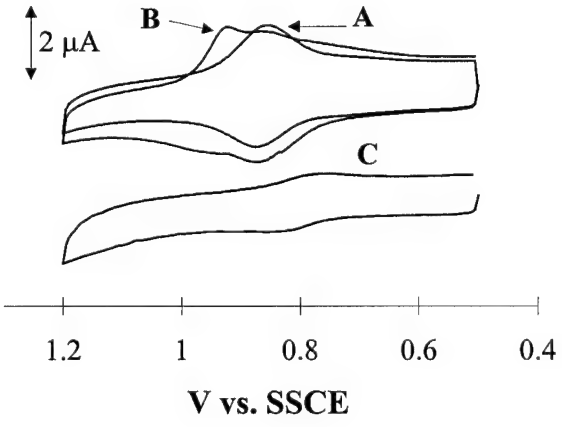

Figure 11. Cyclic voltammograms of A) $[Ru(tpy)(4,4'(PO_3H_2)_2bpy)(H_2O)](ClO_4)_2$ absorbed on ITO. B) With added $Ru^{II}(tpy)(bpy)(H_2O)^{2+}$ at 2.4×10^{-6} M. C). Blank ITO with $Ru^{II}(tpy)(bpy)(H_2O)^{2+}$ added at 2.4×10^{-6} M. The cyclic voltammograms were recorded in 0.1 M $HClO_4$ at a scan rate of 10 mV/s.

These observations are consistent with the intervention of bimolecular reactions in the surface oxidation of Ru^{III}-OH^{2+} to $Ru^{IV}=O^{2+}$. Direct one-electron oxidation of Ru^{III}-OH^{2+} to $Ru^{IV}=OH^{3+}$ is slow or inaccessible because of the high potential for the $Ru^{IV}=OH^{3+}/Ru^{III}$-OH^{2+} couple. Disproportionation (eq 8) followed by Ru^{II}-$OH_2^{2+} \rightarrow$ Ru^{III}-OH_2^{3+} oxidation provides a viable mechanism for surface oxidation.

$$(tpy)(bpy)Ru^{III}\text{-}OH^{2+},\ \underset{\underset{H}{|}}{O}\text{-}Ru^{III}(bpy)(tpy)^{2+} \longrightarrow (tpy)(bpy)Ru^{IV}=O^{2+},\ H\text{-}\underset{\underset{H}{|}}{O}\text{-}Ru^{II}(bpy)(tpy)^{2+} \qquad (8)$$

High surface loadings are required for a mechanism involving proton-coupled electron transfer within an association complex of the reactants. Catalysis of the surface couple by $Ru(tpy)(bpy)(H_2O)^{2+}$ also occurs by proton-coupled electron transfer. In $H_2O/HDO/D_2O$ mixtures with the mole fraction of D(χ_D) varied from 0 to 0.2, the integrated current for the Ru(III→IV) wave varies linearly with χ_D with $k_{H2O}/k_{D2O} = 12.2$, within experimental error of the solution k_{H2O}/k_{D2O} value. The effect of D_2O on the uncatalyzed surface reaction is even more profound. With $\chi_D = 0.05$ in 0.1M $HClO_4$ and full surface coverage there is no discernible Ru(III → IV) wave Figure 12. From data obtained from $\chi_D = 0$ to $\chi_D = 0.025$, and assuming that k varies linearly with χ_D, k_{H2O}/k_{D2O} is equal to or greater than 60.

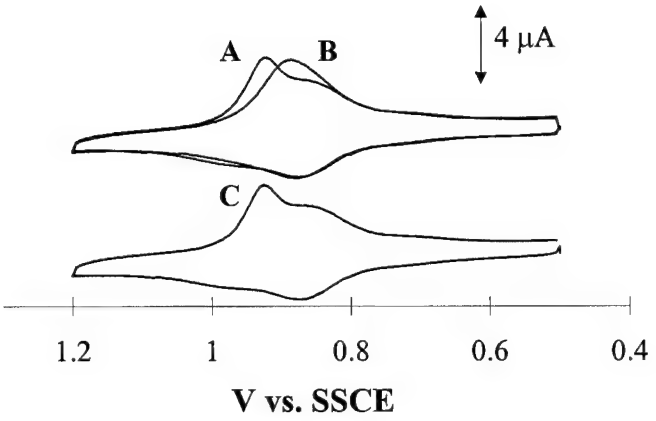

Figure 12. Cyclic voltammograms of A) $[Ru(tpy)(4,4'(PO_3H_2)_2bpy)(H_2O)](ClO_4)_2$ absorbed on ITO in 0.1M $HClO_4$ at a scan rate of 10mV/s B) 5% D_2O, 0.1 M $HClO_4$ C). 0.1M $HClO_4$. The cyclic voltammograms were recorded at a scan rate of 10 mV/s.

The observation of different isotope effects for the surface and solution catalyzed reactions is of fundamental importance. Proton-coupled electron transfer requires specific orientations between reactants for nuclear tunneling of the proton to occur. On the surface, there is a spatial distribution of translationally fixed non-diffusional redox sites and restricted orientations. This must increase the average tunneling distance, increasing the isotope effect.

Electropolymerization

Our studies with reductive electropolymerization on TiO_2 had the immediate goal of creating stable surface structures. Our initial experiments in this area have been carried out in collaboration with Professor Gerald Meyer and his group at Johns Hopkins

University. They have involved pre-adsorbing the mixed acid-vinyl containing complex $[Ru(vbpy)_2(4,4'\text{-}(CO_2H)_2bpy)]^{2+}$ and electropolymerizing an overlayer of *poly*-$[Zn(vbpy)_3]^{2+}$ or *poly*-$[Ru(vbpy)_3]^{2+}$.

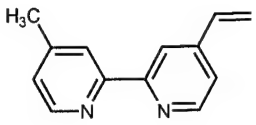

(vbpy)

This is accomplished by scanning the electrode potential from 0 to -1.8 V to 0 in CH_3CN vs. SCE in solutions containing the complex. Reduction into the conduction band of TiO_2 occurs at these potentials. The particles darken and become conductive, but the darkening is reversed by scanning oxidatively.

The degree of overlayer formation depends on the number of reductive scan cycles with 3-4 times the initial monolayer coverage occurring after 30 - 40 cycles with the complex at 1 x 10^{-4} M in 0.1 M $[N(n\text{-}C_4H_9)_4](PF_6)/CH_3CN$. The resulting structures are highly stabilized compared to adsorbed **1** due to the lateral covalent bonding offered by the *poly*-$[Ru(vbpy)_3]^{2+}$ overlayers. The Zn^{II} overlayers are less stable because of the in loss of Zn^{2+} in acidic solution which leads to breakup of the film structures and loss of absorbed film to the solution. As shown by UV-visible absorption measurements, the Ru^{II} structures are stable in water from pH = 0 to pH = 14 for indefinite periods. Reasonable photocurrent efficiencies are obtained photovoltaic cell. The photocurrents of samples with a wide range of film thickness were examined (Figure 13), with the thinnest film (sample J4 - four reduction cycles) having the highest incident photon to current efficiency (IPCE).

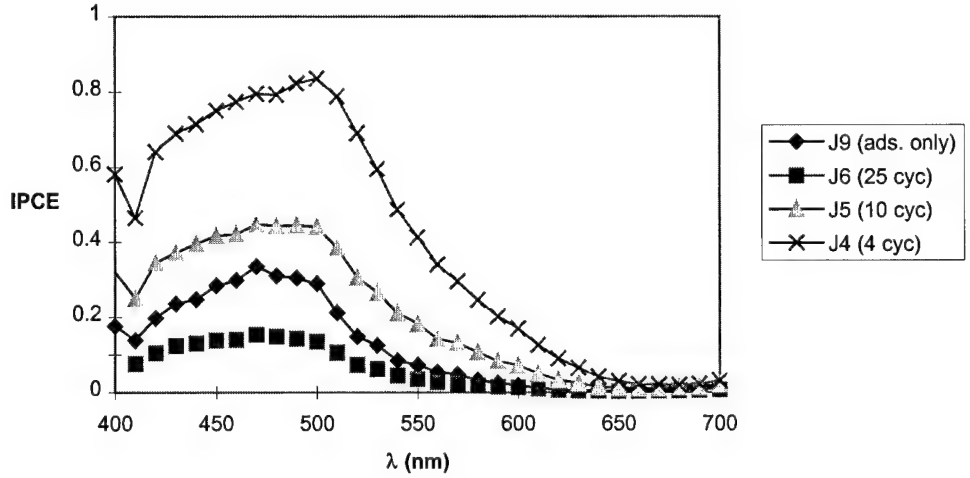

Figure 13. Incident photon to current efficiency (IPCE) of four TiO_2/ITO samples containing adsorbed $Ru^{II}(vbpy)_2(4,4'\text{-}(CO_2H)_2)^{2+}$. J9 has only the adsorbed $Ru^{II}(vbpy)_2(4,4'\text{-}(CO_2H)_2)^{2+}$complex, while J4, J5, and J6 have a varying amount of $Ru(vbpy)_3^{2+}$ with electropolymerized $Ru(vbpy)_3^{2+}$ as an overlayer.

Tapping mode AFM measurements reveal that the electro-polymerized film overlay forms a "blanket " and fills up rough surface features.

We have been able to polymerize films on TiO_2 without the vinyl-containing complex in solution. Electrochemical reduction of TiO_2 films of $[Os^{II}(bpy)_2(4,4'\text{-}(CO_2H)_2)]^{2+}$loaded from CH_3CN suggest that vinyl-containing metal complexes absorbed onto the surface from CH_3CN may be close enough to cause intersite polymerization across the surface of the TiO_2 particle. This is an important result since it may afford stable surface structures without an interfering overlay structure to impede the photoelectrochemical response.

SiO_2 Sol-Gels

Electrochemiluminescence.

One of the focal points in our studies of SiO_2-sol-gel based optical films is their application as electrochemiluminescent coatings. In this regard initial studies were directed to observe electrogenerated chemiluminescence (ECL) from both $Ru(bpy)_3^{2+}$ and $[PS\text{-}CH_2CH_2NHCO\text{-}Ru^{II}_{18})](PF_6)_{36}$ doped SG films. The repeat unit of this polystyrene-derivatized polymer is illustrated below.

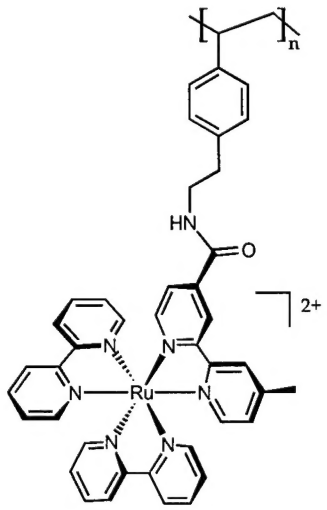

$[PS\text{-}CH_2CH_2NHCO\text{-}Ru^{II}_{18})]^{36+}$

The theory and technical aspects of ECL generation in fluid solution have been described in detail[6]. For generation of ECL in chromophore doped Sol-Gel films we used an approach described as a triple potential step in which the potential applied on the ITO electrode is rapidly switched between the potential corresponding to the $Ru^{3+/2+}$ couple and the potential corresponding to $Ru^{2+/+}$ couple. The electrochemical properties of the $Ru(bpy)_3^{2+}$ in fluid solution and in the SG film and $[PS\text{-}CH_2CH_2NHCO\text{-}Ru^{II}_{18})]^{36+}$ in SG films are summarized in Table 2.

Table 2. Electrochemical properties of $Ru(bpy)_3^{2+}$ and $[PS\text{-}Ru_{18}]^{36+}$ in solution and SG-films. [a]

Sample	$E_{1/2}$, V[b] ($\Delta E = E_{pa} - E_{pc}$)			
	3+/2+ (ΔE)	2+/+ (ΔE)	+/0 (ΔE)	0/- (ΔE)
$Ru(bpy)_3^{2+}$/Solution/ITO	0.97 (120)	-1.64 (120)	-1.85 (130)	-2.12 (120)
$Ru(bpy)_3^{2+}$/SG/ITO	0.94 (130)	c	c	c
$[PS\text{-}CH_2CH_2NHCO\text{-}Ru^{II}_{18})]$/SG/ITO	1.00 (120)	-1.54 (70)	-1.85 (20)	-2.14 (120)

a) 0.1M $[N(n\text{-}C_4H_9)_4](PF_6)$ in CH_3CN
b) V vs. $Ag/AgNO_3$
c) irreversible wave observed

ECL has been monitored for a 1 mmol solution of $Ru(bpy)_3^{2+}$ N; on a bare ITO electrode and for both the $Ru(bpy)_3^{2+}$ and $[PS\text{-}CH_2CH_2NHCO\text{-}Ru^{II}_{18})]^{36+}$ doped SG films (0.1M $[N(n\text{-}C_4H_9)_4](PF_6)$ in CH_3CN). Typically, the potential was pulsed between +1.7V (0.1 s) and -2.0V(0.2 s) (vs. $Ag/AgNO_3$). In all three cases intense an orange luminescence, observable by the naked eye at ambient light is observed. Typically, potential, current and light intensities have been monitored in each experiment. In Figure 14, are shown plots of applied potential with the corresponding current and ECL response for the $[PS\text{-}CH_2CH_2NHCO\text{-}Ru^{II}_{18})]$/SG/ITO film. The current response carries the information about the rate of generation of the reduced ($Ru(bpy)_3^{+}$) and oxidized ($Ru(bpy)_3^{3+}$) species in each pulse step. The intensity of ECL (bottom part of Figure 14) is apparently maximized at the potential change to +1.7V (Ru^{3+} generation). The intensity rapidly decreases within the pulse duration (0.1s) and appears again in another cycle. This gives rise to, a flickering orange luminescence on the electrode surface. ECL is also observed at a higher pulse repetition rate without significant change in the observed ECL intensity. Comprehensive studies of the dependence of the ECL intensity on pulse width and potential step (on both the oxidative and reductive sides) are currently in progress.

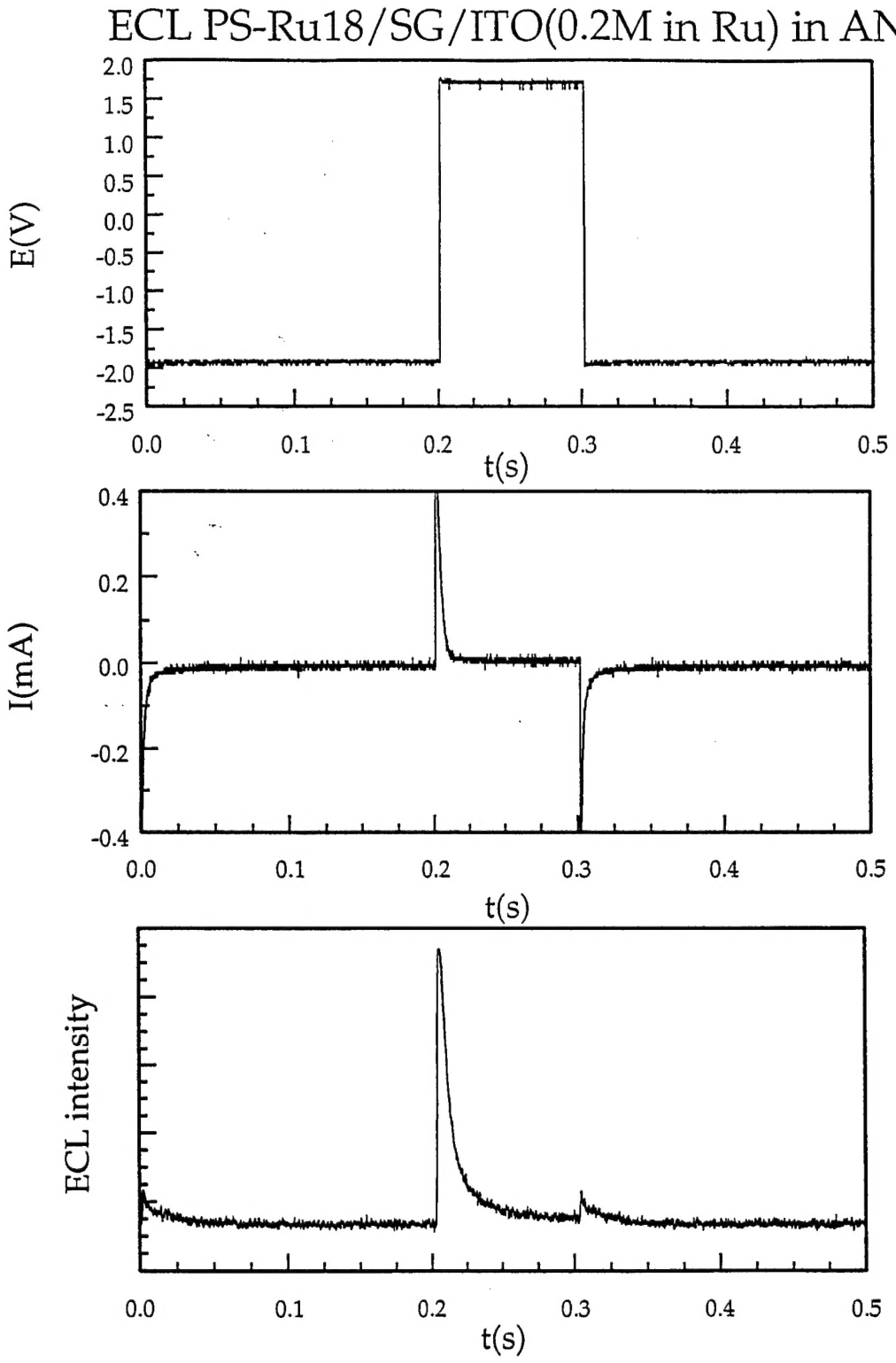

Figure 14. Plots of applied potential with the corresponding current and ECL response for the [PS-Ru_{18}]/SG/ITO film.

Bibliography

1. Trammell, S.; Meyer, T. J. *Manuscript in Preparation* **1997**.

2. Trammell, S.; Meyer, T. J. submitted to *Inorg. Chem.* **1998**.

3. Takeuchi, K. J.; Thompson, M. S.; Pipes, D. W.; Meyer, T. J. *Inorg. Chem.* **1984**, *23*, 1845-1851.

4. Péchy, P.; Rotzinger, F. P.; Nazeeruddin, M. K.; Kohle, O.; Zakeeruddin, S. M.; Humphry-Baker, R.; Grätzel, M. *Chem. Commun.* **1995**, 65-66.

5. Trammell, S.; Wimbish, J.; Meyer, T. J. submitted to *J. Am. Chem. Soc.* **1998**.

6. Bard, A. J.; Faulkner, L. R. *Electrochemical Methods - Fundamentals and Applications*; John Wiley & Sons, Inc.: New York, 1980.